Supporting Information

A facile phase transformation-mediated mechanochemical assembly strategy facilitates scale up synthesis of enzyme@MOF biocomposites

Qing Chen,[a] Lihong Guo,[a,b] Xiaoxue Kou,[a] Rui Gao,[a] Ningyi Zhong,[a] Anlian Huang,[a] Rongwei He,[a,b] Siming Huang,*[c] Fang Zhu,[a] Guosheng Chen*[a] and Gangfeng Ouyang[a]

[a]MOE Key Laboratory of Bioinorganic and Synthetic Chemistry, School of Chemistry, Sun Yat-sen University, Guangzhou 510006, China

[b]Instrumental Analysis and Research Center, Sun Yat-sen University, Guangzhou 510275, China

[c]Guangzhou Municipal and Guangdong Provincial Key Laboratory of Molecular Target & Clinical Pharmacology, the NMPA and State Key Laboratory of Respiratory Disease, School of Pharmaceutical Sciences and the Fifth Affiliated Hospital, Guangzhou

*Corresponding authors, E-mail: hangsm@gzhmu.edu.cn (S. Huang); chengsh39@mail.sysu.edu.cn (G. Chen)

Supplemental Experimental Procedures

Reagent and materials.

Lipase PS and nano-zinc oxide (ZnO) were purchased from Aladdin Chemistry Co., Ltd. (Shanghai, China). Triphenylene-2,3,6,7,10,11-hexaol (HHTP) and 2-methylimidazole (HmIM) were obtained from J&K Scientific (Beijing, China). Lipase from *Thermomyces lanuginosus* (TL) was supplied by Novozymes (Beijing, China). Notably, the raw TL was subjected to dialysis (molecular weight cut-off, MWCO = 3 kDa) to remove impurities and salts, followed by lyophilization prior to use. *p*-Nitrophenyl butyrate (*p*-NPB) and *p*-nitrophenol (*p*-NP) were obtained from Macklin Biochemical Technology Co., Ltd. (Shanghai, China). Bicinchoninic acid (BCA) assay reagents, Tris buffer, and HAc buffer were purchased from Shanghai Yuanye Bio-Technology Co., Ltd. (Shanghai, China). All chemicals and reagents were obtained from commercial sources and used without further purification.

Characterization.

Powder X-ray diffraction (PXRD) patterns were recorded using a Bruker D8 Advance diffractometer (Cu Kα radiation) at room temperature, with data collected at a step size of 0.02° and a dwell time of 0.06 s per step. Ultraviolet-visible (UV-vis) absorbance measurements were conducted using a 2800S spectrophotometer (SOPTOP, Shanghai). Fourier transform infrared (FT-IR) spectra were acquired using a Bruker EQUINOX 55 spectrometer with 32 scans over a spectral range of 4000–400 cm^{-1}. Morphological characterization was performed using a SU8010 ultrahigh-resolution field-emission scanning electron microscope (SEM, Hitachi, Japan), with dried samples sputter-coated with gold prior to imaging. Transmission electron microscopy (TEM) and energy-dispersive X-ray spectroscopy (EDS) mapping were carried out using a JEM-ARM200P spherical aberration-corrected TEM operated at 200 kV. TEM samples were prepared by drop-casting 5 μL of diluted samples onto formvar carbon-coated copper grids.

N_2 adsorption isotherms were measured using a JW-DX surface area analyzer, with samples pretreated at 120 °C for 12 h prior to measurement. The total pore volume was determined using the Barrett–Joyner–Halenda (BJH) method. Thermogravimetric analysis (TGA) was conducted under an N_2 atmosphere (20 mL/min) with a heating rate of 10 °C/min using a TA-Q50 system. Confocal laser scanning microscopy (CLSM 880 NLO, Carl Zeiss, Göttingen, Germany) was employed to visualize the distribution of dye-labeled enzymes within MOFs and ZIF-8. Circular dichroism (CD) spectra of enzymes were recorded using a J1700 CD spectrometer (JASCO, Japan) over a wavelength range of 190–400 nm. The enzymes

quantification was operated on a microplate reader (Cytation 3, BioTek, USA). Fluorescence spectra of TL were obtained using an RF-5301PC fluorescence spectrometer (Shimadzu, Japan).

Mechanochemical synthesis of TL@Zn-HHTP through the PTME method.

The mechanochemical synthesis of TL@Zn-HHTP was performed under optimal conditions using a planetary ball mill (PMQW2, ChiShun, China) with 25 mL zirconia jars containing ten zirconia balls (3.5 mm in diameter) and seventy zirconia balls (1 mm in diameter). In a typical procedure, TL (5 mg), nano-zinc oxide (ZnO, 10 mg), and HHTP (20 mg) were placed into a zirconia jar. Subsequently, 35 μL of 500 mM Tris buffer (pH 7.4) or HAc buffer (pH 6.0) was added as catalysts to facilitate mechanical milling. The mixture was ground at a rotational speed of 550 rpm for 1 min at room temperature. The resulting samples were collected, washed three times with deionized water, and stored at 4 °C. For the synthesis of Zn-HHTP, the enzyme was omitted, while all other experimental conditions remained identical to those used for TL@Zn-HHTP.

Mechanochemical synthesis of TL@ZIF-8 through the PTME method.

The mechanochemical synthesis of TL@ZIF-8 was conducted using a planetary ball mill under optimized conditions. In a typical procedure, nano-ZnO (10 mg), 2-methylimidazole (HmIM, 20 mg), and TL (5 mg) were placed into a zirconia jar containing ten zirconia balls (3.5 mm in diameter) and seventy zirconia balls (1 mm in diameter). Subsequently, 35 μL of 500 mM Tris buffer (pH 7.4) or HAc buffer (pH 6.0) was added as the catalysts, and the mixture was milled at a rotational speed of 550 rpm for 1 min. The resulting samples were collected, washed three times with deionized water, and stored at 4 °C.

Mechanochemical synthesis of PS@Zn-HHTP through the PTME method.

The mechanochemical synthesis of PS@Zn-HHTP was conducted using a planetary ball mill under optimized conditions. In a typical procedure, nano-ZnO (10 mg), HHTP (20 mg), and PS (5 mg) were placed into a zirconia jar containing ten zirconia balls (3.5 mm in diameter) and seventy zirconia balls (1 mm in diameter). Subsequently, 35 μL of 500 mM Tris buffer (pH 7.4) or HAc buffer (pH 6.0) was added as the catalysts, and the mixture was milled at a rotational speed of 550 rpm for 1 min. The resulting samples were collected, washed three times with deionized water, and stored at 4 °C.

Mechanochemical synthesis of Cutinase@Zn-HHTP through the PTME method.

The mechanochemical synthesis of Cutinase@Zn-HHTP was performed under optimized conditions using a planetary ball mill. In a typical procedure, nano-ZnO (10 mg), HHTP (20 mg), and Cutinase (5 mg) were placed into a zirconia jar containing ten zirconia balls (3.5 mm in diameter) and seventy zirconia balls (1 mm in diameter). Subsequently, 35 μL of 500 mM Tris buffer (pH 7.4) or HAc buffer (pH 6.0) was added as an assisting liquid, and the mixture was milled at a rotational speed of 550 rpm for 1 min. The resulting samples were collected, washed three times with deionized water, and stored at 4 °C.

Hydrothermal method of TL@Zn-HHTP.

For comparison, TL was also encapsulated into Zn-HHTP using a previously reported hydrothermal method.[1] In a typical procedure, zinc acetate (6.8 mg, 0.037 mmol) was dissolved in 4 mL of water and stirred at 85 °C for 10 min. Subsequently, TL (4 mg) and 1 mL of 0.25 M sodium acetate aqueous solution were added, followed by the immediate addition of HHTP (13 mg, 0.024 mmol). The reaction mixture was stirred at 85 °C for 2 h. The resulting precipitate was collected by centrifugation (10,000 rpm, 5 min) and washed three times with deionized water.

Measurement of TL and Cutinase loading

The loading content of TL and Cutinase in enzyme@Zn-HHTP and enzyme@ZIF-8 was determined by measuring the enzyme concentration in the supernatants before and after encapsulation using a standard Bicinchoninic Acid (BCA) assay. 20 μL of enzyme sample was transferred to a 96-well plate, and 200 μL of BCA reagent was added to each well. The mixture was incubated at room temperature for 30 minutes, after which the absorbance at 562 nm was measured using a microplate reader. The enzyme concentration was calculated based on the absorbance values at 562 nm through a standard curve method.

Measurement of PS loading

As PS cannot be quantified using the BCA assay, we employed a UV-Vis assay to estimate the PS loading content of PS@Zn-HHTP. A series of PS solutions with concentrations of 0.05, 0.1, 0.5, 1, and 2 mg/mL were prepared. In this assay, 5 μL of 100 mM p-NPB, 975 μL of 50 mM Tris buffer (pH 8.0), and 20 μL of free PS enzyme at different concentrations were mixed in a cuvette. The enzyme concentration is proportional to the rate of change in UV absorption at 405 nm. Plotting the PS concentration against the

rate of change in absorbance at 405 nm provides a calibration curve, which can be used to determine the PS concentration in the supernatants before and after encapsulation.

Fluorescence labeling of TL.

Fluorescence labeling experiments were conducted based on the conjugation between the amino group of the lysine residue in TL and the thiocarbamide group of the fluorescent dye. In brief, 20 mg of TL was dispersed in 1 mL of carbonate buffer solution (pH 9.0, 0.5 M), followed by the addition of 1 mg of rhodamine B (RhB) isothiocyanate. The resulting mixture was stirred for 12 hours in the dark. Finally, RhB-labeled TL was purified through ultrafiltration using a centrifugal filter device (molecular weight cut-off MWCO = 8 kDa) to remove excess reagents and salts.

CLSM experiment

In the CLSM experiment, the original TL was replaced with RhB-labelled TL to prepare TL@Zn-HHTP biocomposites. The TL@Zn-HHTP samples were dissolved in ethanol, and the resulting solution was deposited onto a 35 mm glass-bottom dish. The samples were dried under vacuum to complete the preparation. The fluorescence of the TL@Zn-HHTP biocomposites was excited at a wavelength of 562 nm using a confocal laser scanning microscope. For Z-scan imaging, the slice parameter was set to 200 nm per step.

Examinations of enzymatic activities.

The enzymatic activities of free enzymes (TL, PS, and Cutinase) and enzyme@MOFs were evaluated using p-NPB (4C) as the ester substrate. TL, PS, and Cutinase catalyze the hydrolysis of p-NPB (4C), producing yellow p-nitrophenol (p-NP) as the product. The activity assay was performed as follows: free enzymes or enzyme@MOFs were added to a cuvette containing Tris-HCl buffer (50 mM, pH 8.0). A series of substrate concentrations (final concentrations of 0.01, 0.04, 0.08, 0.1, 0.5, and 1.0 mg/mL) were introduced to initiate the catalytic reaction. Notably, the final enzyme concentration (5 μg/mL) was kept constant for both free enzymes and enzyme@MOFs. The formation of yellow p-NP was monitored at 405 nm using a UV-vis spectrophotometer, and its concentration was determined based on a standard calibration curve (Fig. S11).

Measurement of the catalytic kinetic parameters

The catalytic kinetic parameters were measured according to the Michaelis-Menten equation:

$$V_0 = \frac{V_{max}[S]}{K_m + [S]}$$

Here, V_0 represents the initial catalytic rate, while V_{max} denotes the maximum rate of conversion, achieved when the catalytic sites on the TL are saturated with substrate. [S] represents the initial substrate concentration, and K_m is the Michaelis-Menten constant. The initial catalytic rate V_0 was determined by calculating the slope of the kinetic curve during the initial phase, and the initial substrate concentration [S] was determined at t = 0 s. The kinetic parameters K_m and V_{max} were fitted using a Michaelis-Menten equation, based on the calculated V_0 and [S].

Evaluation of adsorption capacity of Zn-HHTP toward TL.

In this experiment, 2 mg of TL was added to 2 mL of a dispersed Zn-HHTP solution (1 mg/mL). After stirring the mixture for 30 minutes, the enzyme adsorption onto Zn-HHTP was assessed by measuring the concentration change in the supernatant before and after adsorption.

Recyclability Tests.

In the recyclability tests, a TL@Zn-HHTP suspension with an enzyme concentration of 0.25 mg/mL and 100 mM p-NPB was prepared. First, 200 μL of the 0.25 mg/mL TL@Zn-HHTP suspension was added to 799 μL of tris-buffer (50 mM, pH 8), followed by the addition of 1 μL of p-NPB to initiate the catalytic reaction. After 30 seconds, the catalytic product was monitored by UV-vis spectroscopy at 405 nm. The TL@Zn-HHTP catalyst was then collected by centrifugation and washed with deionized water to remove residual products and unreacted p-NPB.

To evaluate recyclability, the collected TL@Zn-HHTP was reused for subsequent catalysis under the same experimental conditions. The change of absorbance intensity at 405 nm relative to the first run was used to evaluate the recyclability.

Supplementary Tables

Table S1. The loading contents of enzymes in different MOFs by the PTME and hydrothermal

methods.

Sample	loading (w/w %)
TL@Zn-HHTP (PTME method)	12.0
PS@Zn-HHTP (PTME method)	12.2
Cutinase@Zn-HHTP (PTME method)	12.6
TL@ZIF-8 (PTME method)	14.3
TL@Zn-HHTP (hydrothermal method)	32.5

Table S2. The summarized catalytic kinetic parameters for PS and Cutinase.

Sample	V_{max} (mM/s)	K_m (mM)	K_{cat} (s^{-1})	K_{cat}/K_m ($(mM \cdot s)^{-1}$)
Free PS	1.24	0.35	3.54	10.11
PS@Zn-HHTP	1.40	0.35	4.00	11.43
Free Cutinase	4.13	0.19	21.7	114.4
Cutinase@Zn-HHTP	3.84	0.25	15.4	61.44

Table S3. The catalytic kinetic parameters of TL@Zn-HHTP synthesized by hydrothermal method.

Sample	V_{max} (mM/s)	K_m (mM)	K_{cat} (s^{-1})	K_{cat}/K_m ($(mM \cdot s)^{-1}$)
TL@Zn-HHTP (hydrothermal method)	1.89	0.85	2.22	2.62

Table S4. Overview of reaction optimizations for Zn-HHTP synthesis by the PTME method.

Entry	Reactant		Liquid additive				Time	Zn-HHTP
	ZnO (mg)	HHTP (mg)	Solvent	Amount (uL)	Concentration (mM)	pH	(min)	conv.(%)
S1	5	20	DI water	20	/	/	60	>98%.
S2	10	20	DI water	20	/	/	15	0%
S3	10	20	DI water	20	/	/	30	0%
S4	10	20	DI water	20	/	/	60	>98%.
S5	5	30	DI water	40	/	/	60	partial
S6	5	40	DI water	40	/	/	60	partial
S7	10	10	DI water	20	/	/	60	0%
S8	10	20	Ethanol	20	/	/	60	0%
S9	10	20	HAc buffer	35	500	5.0	1	>98%.
S10	10	20	HAc buffer	35	500	6.0	0.5	>98%.
S11	10	20	HAc buffer	35	500	6.0	1	>98%.
S12	10	20	HAc buffer	35	500	6.0	2	>98%.
S13	10	20	HAc buffer	35	500	6.0	5	>98%.
S14	10	20	Tris buffer	35	500	7.4	0.5	partial
S15	10	20	Tris buffer	35	500	7.4	1	>98%.
S16	10	20	Tris buffer	35	500	7.4	2	>98%.
S17	10	20	Tris buffer	35	500	7.4	5	>98%.
S18	10	20	Tris buffer	35	500	8.0	1	>98%.
S19	10	20	NaOH	35	/	8.0	1	0%
S20	10	20	HCl	35	/	6.0	1	0%
S21	10	20	Sodium acetate	35	500	/	1	partial
S22	10	20	Acetic acid	35	500	/	1	partial
S23	10	20	Formic acid	35	500	/	1	>98%.
S24	10	20	Formic acid	35	/	5.0	1	>98%.
S25	10	20	Benzoic acid	35	500	/	1	>98%.
S26	10	20	Benzoic acid	35	/	5.0	1	>98%.
S27	10	20	Iso-phthalic acid	35	500	/	1	partial
S28	10	20	Iso-phthalic acid	35	/	5.0	1	partial
S29	10	20	Trimesic acid	35	500	/	1	>98%
S30	10	20	Trimesic acid	35	/	5.0	1	>98%.

Table S5. Detailed performances comparison of TL@Zn-HHTP synthesized by the PTME and hydrothermal methods.

Item	TL@Zn-HHTP (PTME method)	TL@Zn-HHTP (Hydrothermal method)	TL@ZIF-8 (PTME method)
Reaction time (minute)	1.0	120.0	1.0
Volume of solvent (mL)	0.035	10	0.035
[a]Atom efficiency (%)	94.6	74.9	92.6
K_{cat} (s^{-1})	3.39	2.22	1.08
V_{max} (mM/s)	4.14	1.89	2.39
Temperature (ºC)	25.0	85.0	25.0
[b]PMI	2.19	264.06	2.39

[a]The calculation method for atom economy: $\frac{\text{The total mass of the expected product}}{\text{The total mass of the product}} * 100\% = \text{Atom efficiency}\%$

[b]The calculation method for process mass intensity (PMI): $\frac{\text{Total mass of all input materials}}{\text{Mass of the target product}} = PMI$

Table S6. The temperature variation of ball mill jar before and after mechanochemical synthesis.

	Before grinding (ºC)	After grinding (ºC)	Variation (ºC)	Mean variation (ºC)
Zn-HHTP (1min)			0.4	0.37
			0.4	
			0.3	
Zn-HHTP (60 min)			0.5	0.47
			0.5	
			0.4	

			-0.4	
ZIF-8 (1min)			-0.5	-0.43
			-0.4	

Note：We estimated the temperature changes during the reaction by using an infrared thermometer to measure the temperature of the materials inside the ball mill jar before and after the reaction. The results indicated that the temperature remained almost unchanged, even after ball milling for 1 hour. This is because the mechanical energy from the high-speed rotation of the balls was converted into the energy required for the reaction and a small portion of internal energy, with a minor fraction of this internal energy being dissipated to the surrounding environment through heat loss. Thus, we concluded that the actual reaction temperature was near ambient temperature of 25°C.

Supplementary Figures

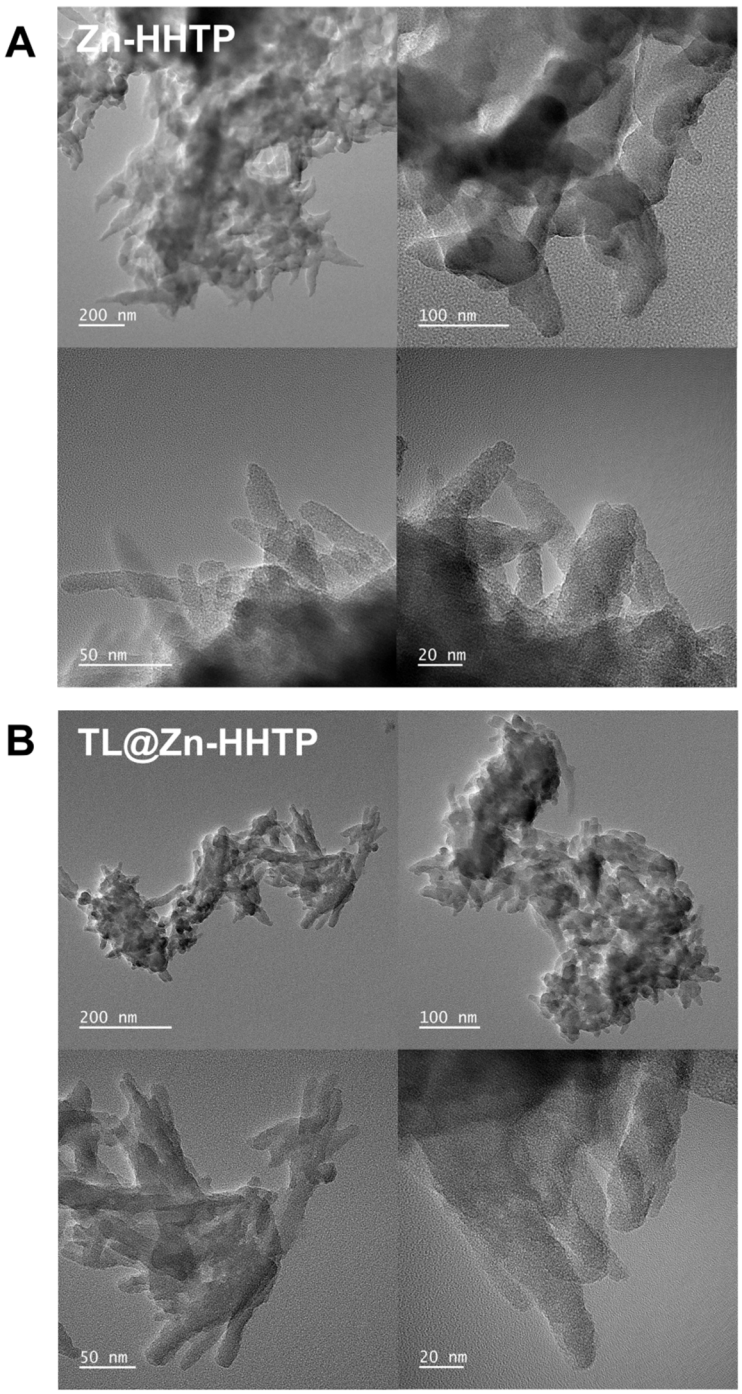

Figure S1. TEM images of (A) Zn-HHTP and (B) TL@Zn-HHTP.

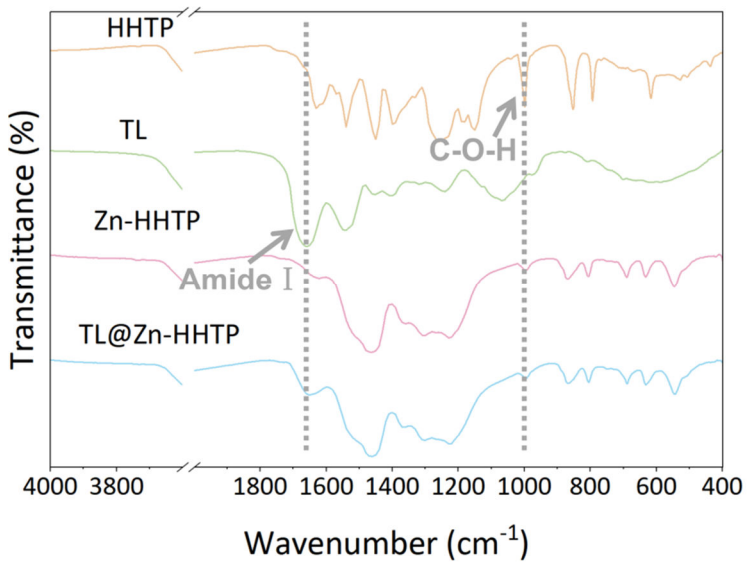

Figure S2. FT-IR spectra of the HHTP, TL, Zn-HHTP, and TL@Zn-HHTP.

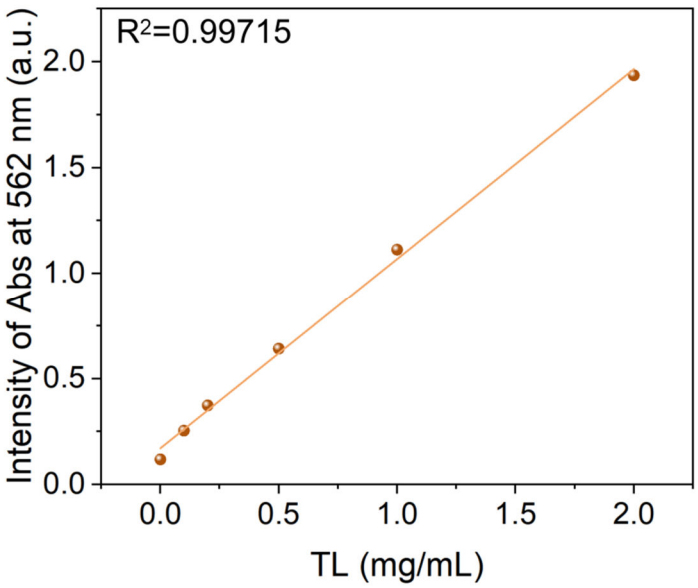

Figure S3. The calibration curve of TL based on BCA method.

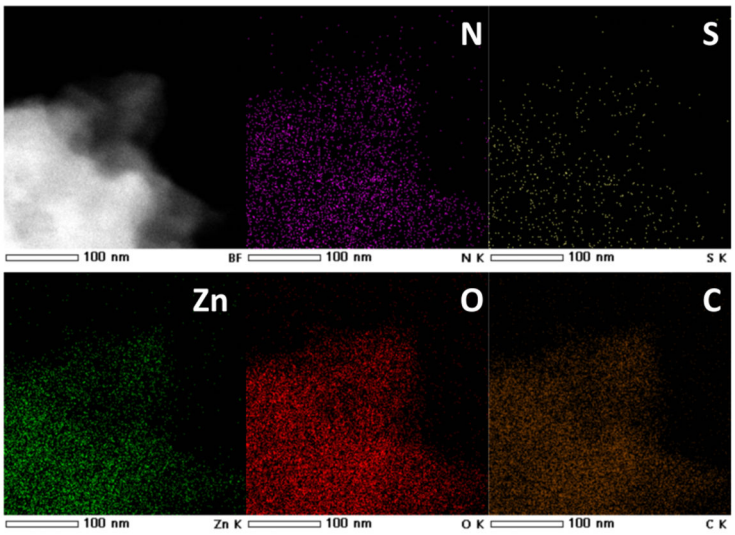

Figure S4. Bright-field image and EDS elemental mapping for TL@Zn-HHTP. Scale bar, 100 nm.

The EDS analysis revealed the presence of Zn, O, C, N, and S elements in TL@Zn-HHTP samples. Among them, Zn, O, and C originate from Zn-HHTP, while S and N are derived from the lipase TL. The uniform distribution of S and N elements indicated that TL was uniformly distributed within the materials.

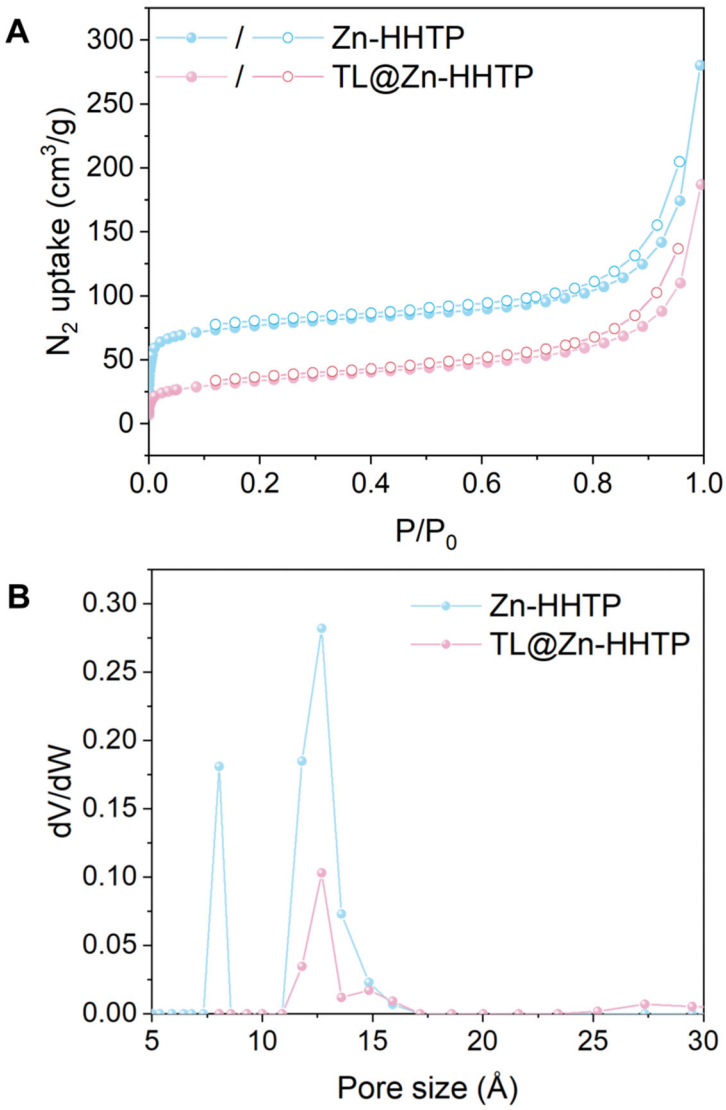

Figure S5. N_2 adsorption-desorption isotherms (A) and the corresponding pore size distributions (B) of Zn-HHTP and TL@Zn-HHTP.

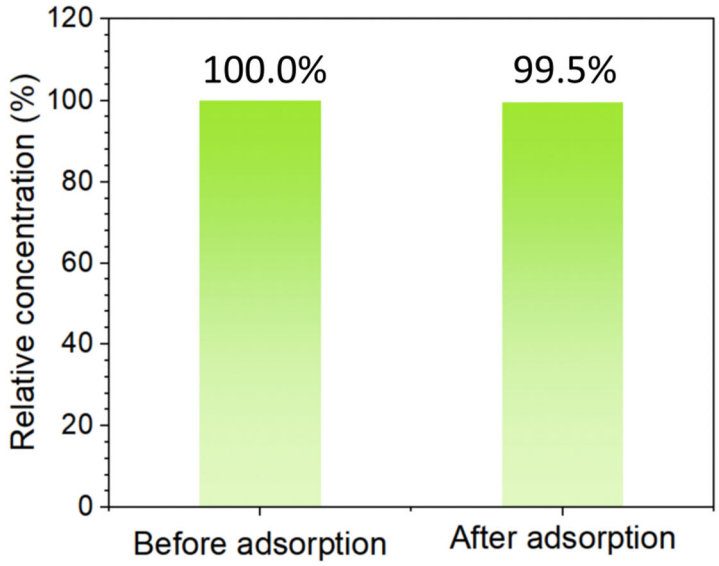

Figure S6. UV-visible spectrum presenting the limiting adsorption capacity of Zn-HHTP for TL.

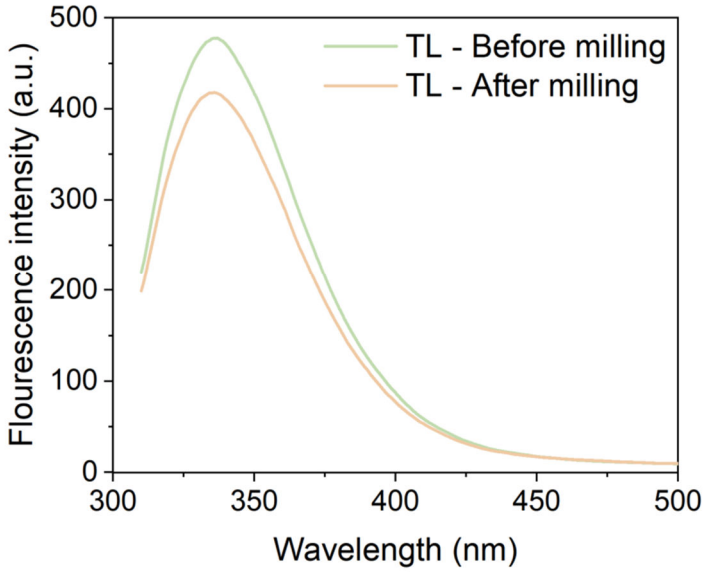

Figure S7. Fluorescence spectra of TL before and after mechanically milling (under 35 μL 500 mM pH 6.0 HAc buffer) treatment for one minute.

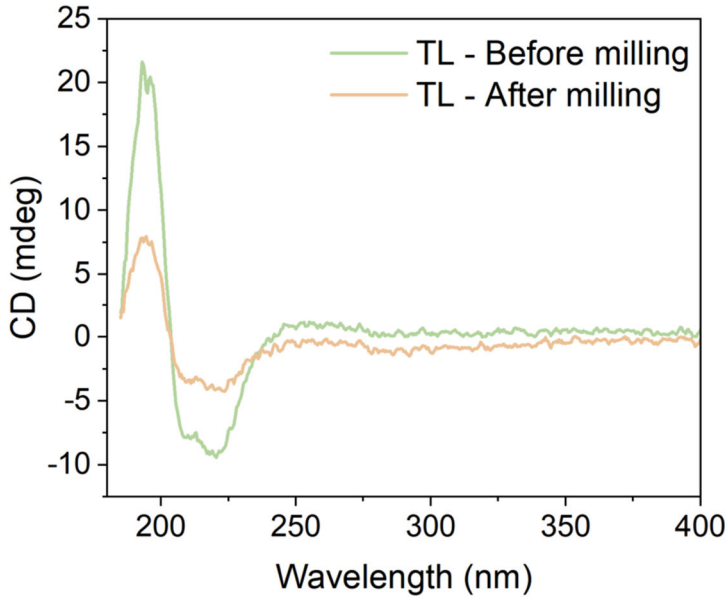

Figure S8. Circular dichroism (CD) spectra of TL before and after mechanically milling (under 35 μL 500 mM pH 6.0 HAc buffer) treatment for one minute.

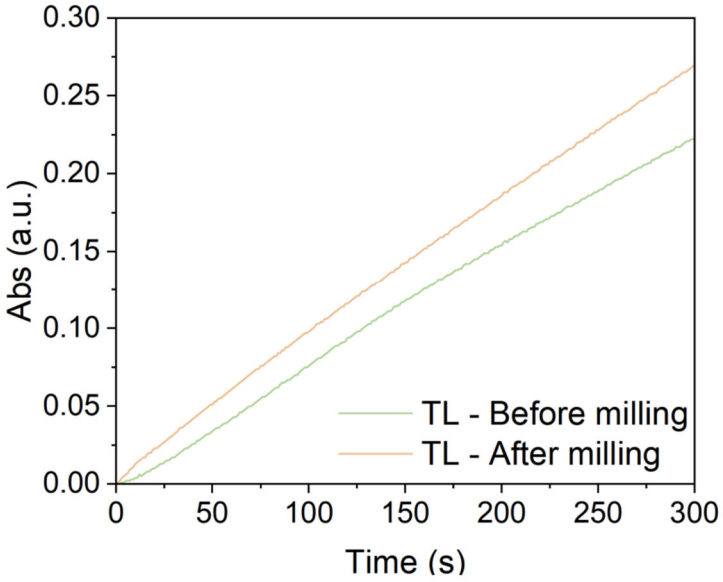

Figure S9. The catalytic kinetics curves of TL before and after mechanically milling (under 35 μL 500 mM pH 6.0 HAc buffer) for one minute.The results showed that the mechanically milling in our assembling system could not affect the bioactivity of the enzyme.

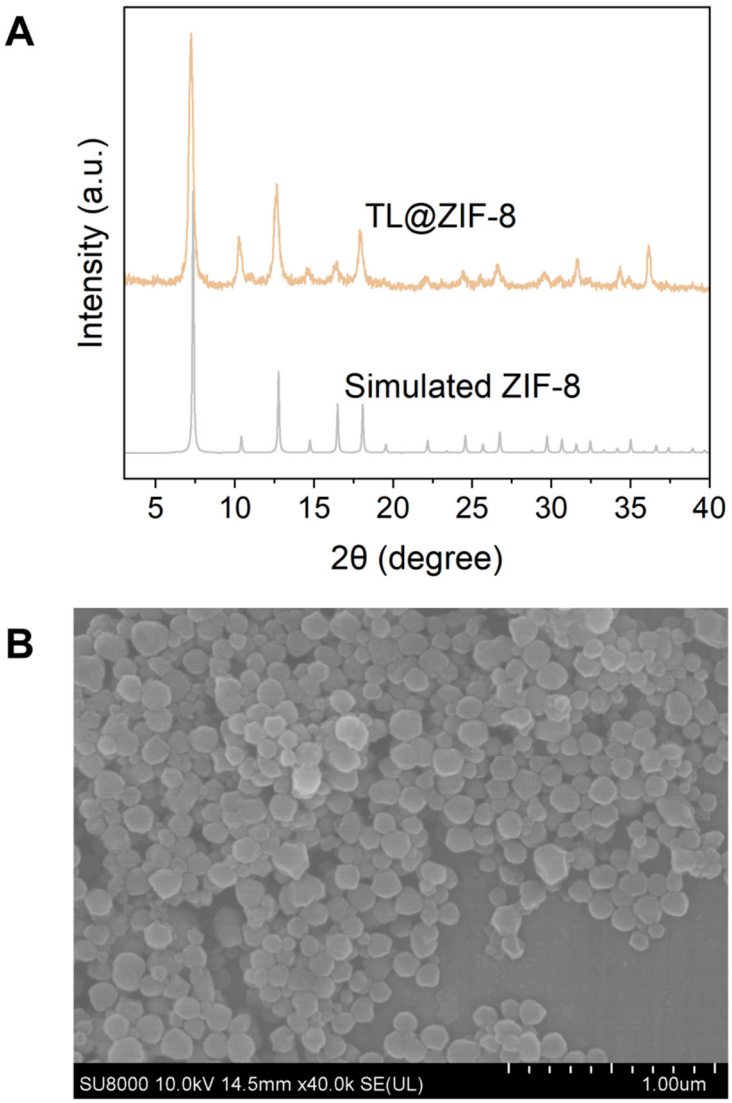

Figure S10. The PXRD (A) and SEM images (B) of prepared TL@ZIF-8 through our PTME method.

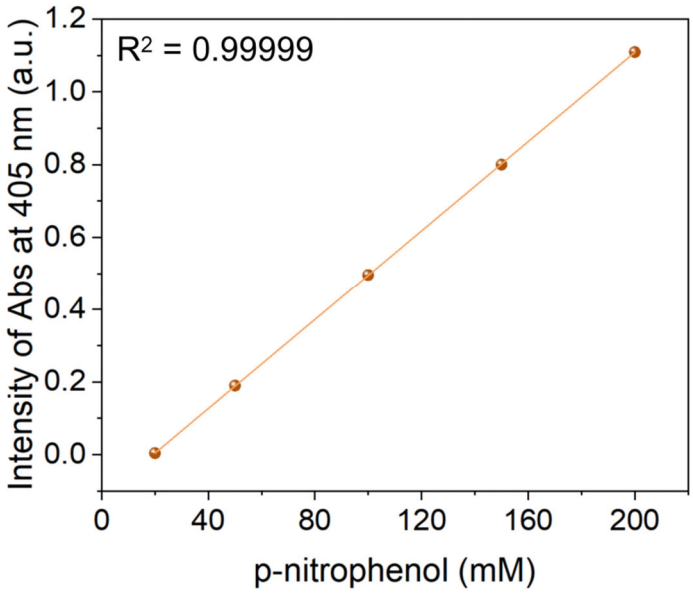

Figure S11. The linear relationship between p-nitrophenol concentration and absorbance at 405 nm.

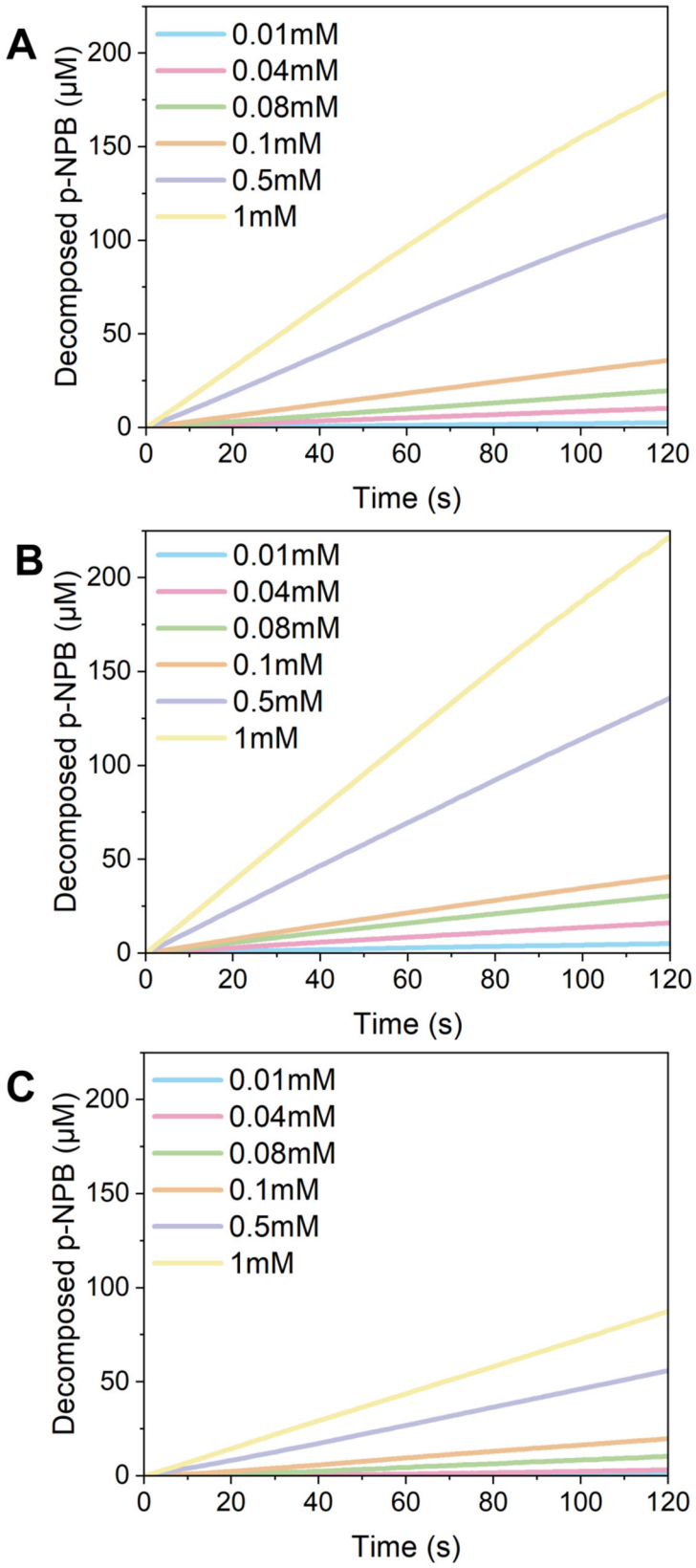

Figure S12. The catalytic kinetics curves of (A) TL, (B) TL@Zn-HHTP and (C) TL@ZIF-8 under different concentrations of substrate [p-NPB]. The dosages of TL (5 μg/mL) were kept the same in each trial.

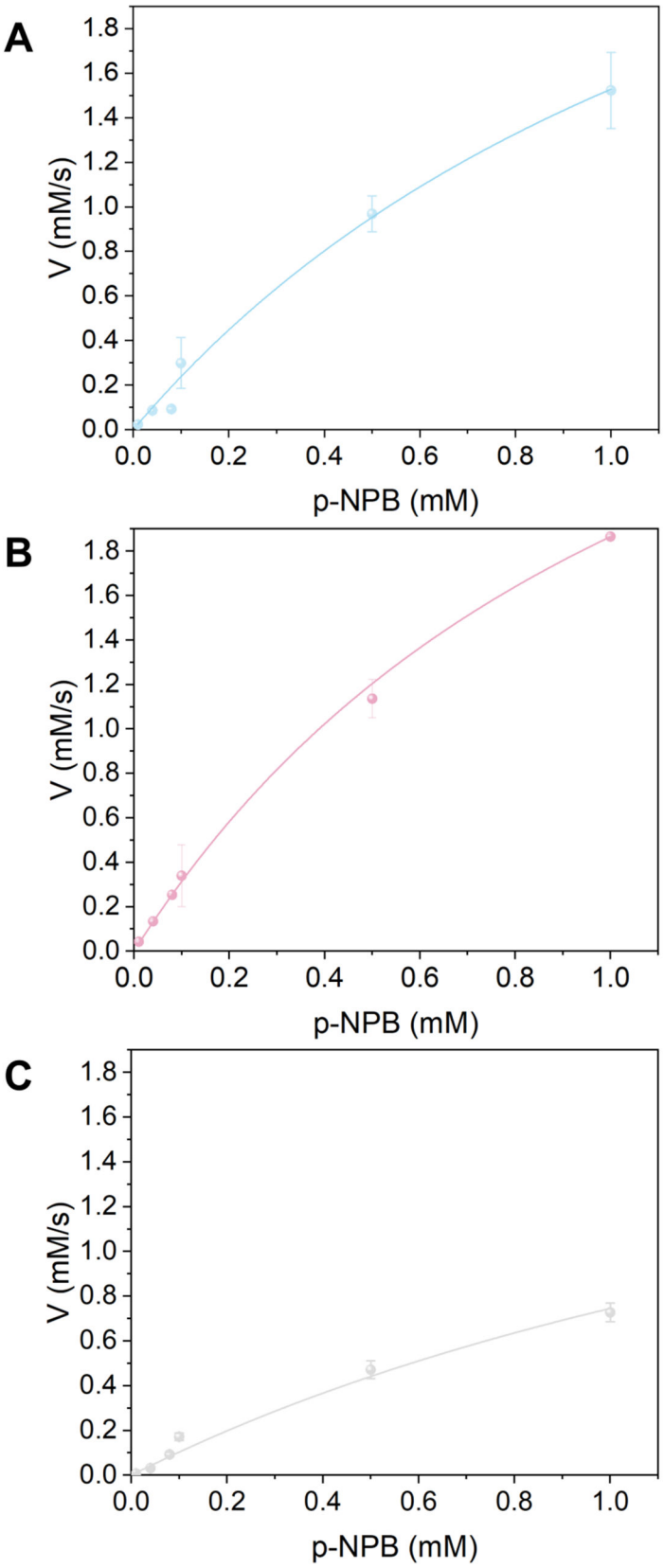

Figure S13. (A) Plot of reaction velocity, V, against substrate [p-NPB] for (A) TL, (B) TL@Zn-HHTP and (C) TL@ZIF-8. The error bars are representative of the standard deviation of the triplicates. The dosages of TL (5 μg/mL) were kept the same in each trial.

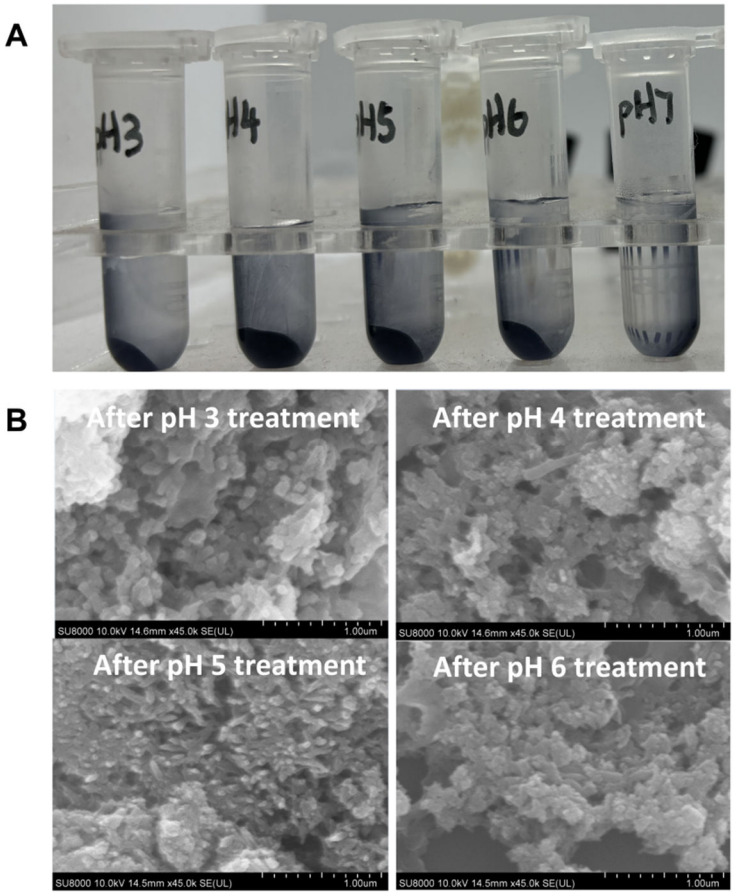

Figure S14. The real photo (A) and SEM images (B) of TL@Zn-HHTP soaked in acidic solutions with different pH values for 2 hours.

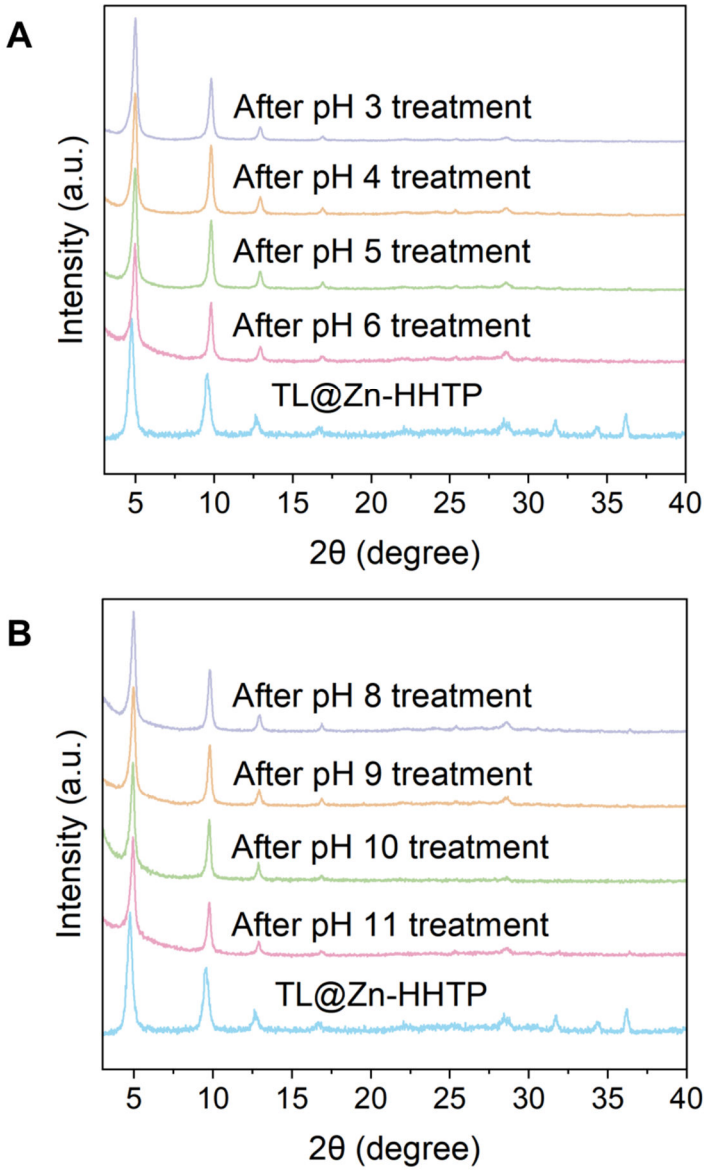

Figure S15. PXRD of (A) TL@Zn-HHTP after acidic (A) and alkaline (B) water solutions treatment for 2 hours.

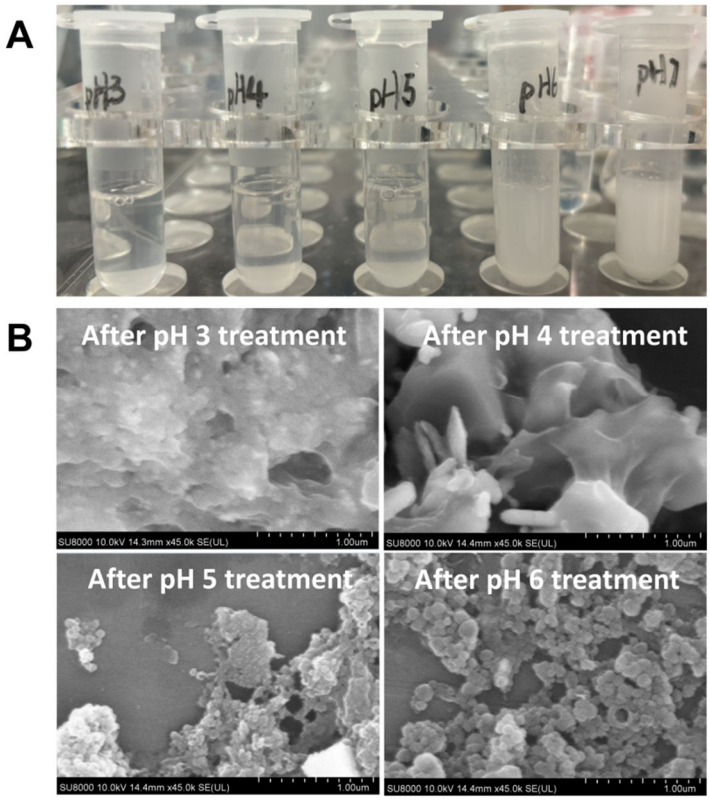

Figure S16. The real photo (A) and SEM images (B) of TL@ZIF-8 soaked in acidic solutions with different pH values for 2 hours.

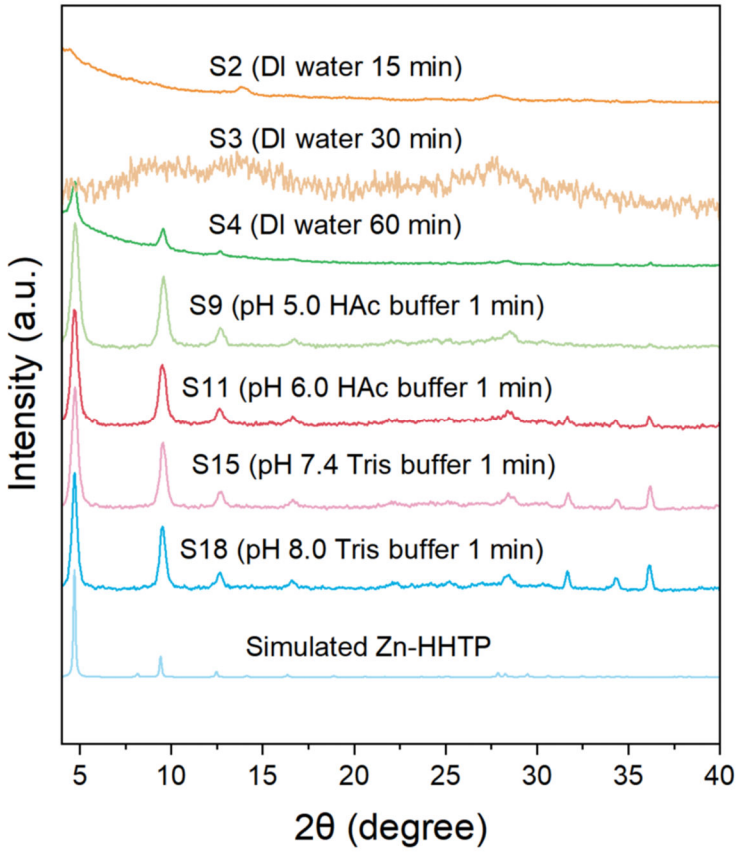

Figure S17. PXRD patterns for the representative Zn-HHTP samples (entries S1-S4, S9, S11, S15, S18 in Table S4), of which the reaction buffer and time are highlighted in bracket. More details of the reaction conditions can be found in Table S4.

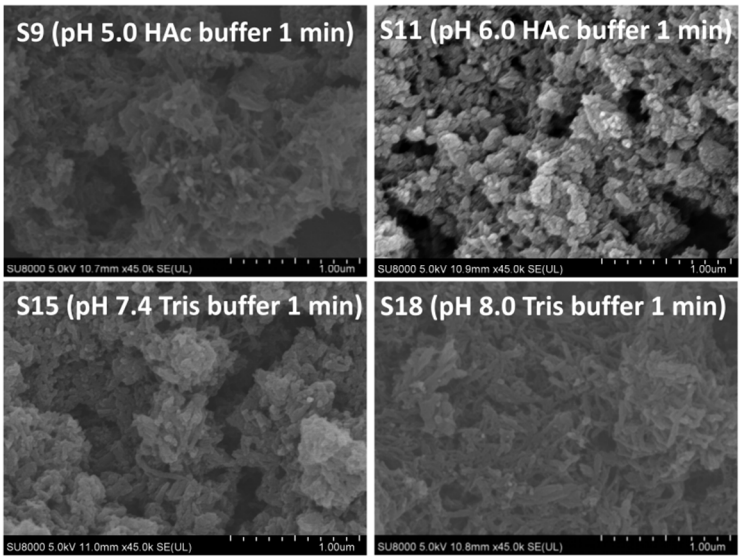

Figure S18. The SEM images for the representative Zn-HHTP samples (entries S9, S11, S15, S18 in Table S4), of which the reaction buffer and time are highlighted in bracket. More details of the reaction conditions can be found in Table S4.

The SEM images reveal that the Zn-HHTP synthesized under different pH buffer conditions are all in an aggregated state, accompanied by short nanorods.

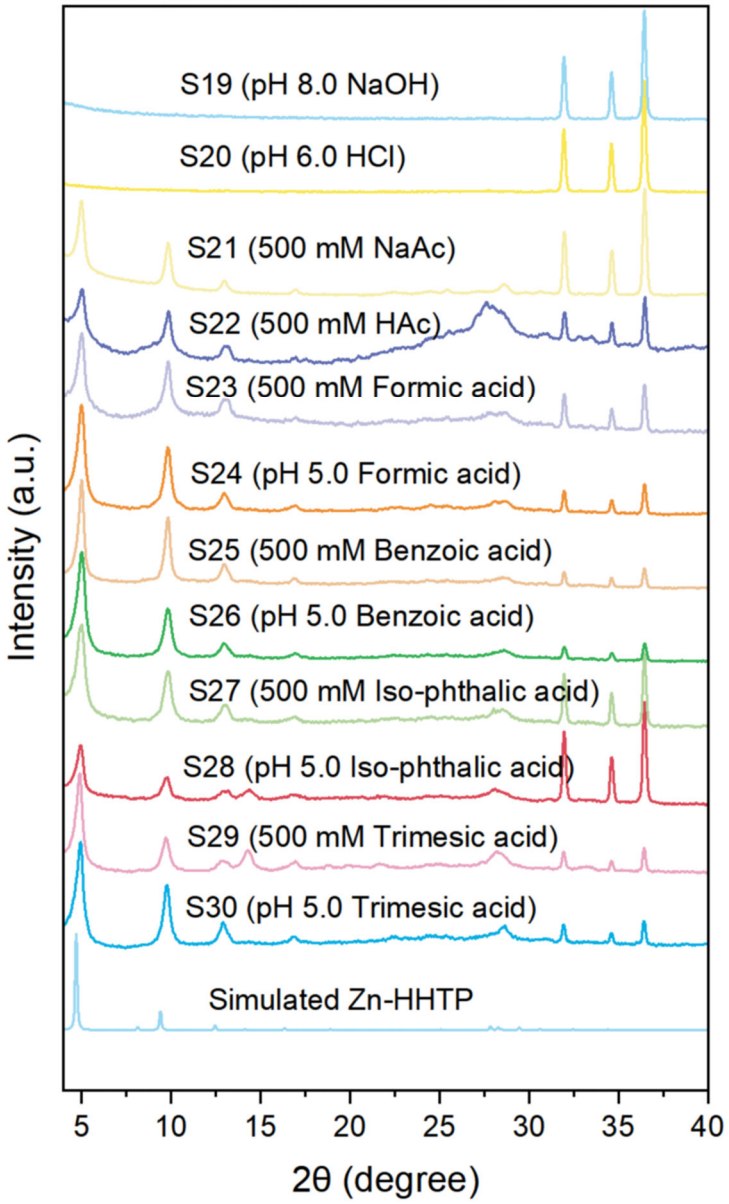

Figure S19. PXRD patterns for the representative Zn-HHTP samples (entries S19-S30 in Table S4), of which the pH or concentration conditions of the reaction additive are highlighted in bracket. More details of the reaction conditions can be found in Table S4.

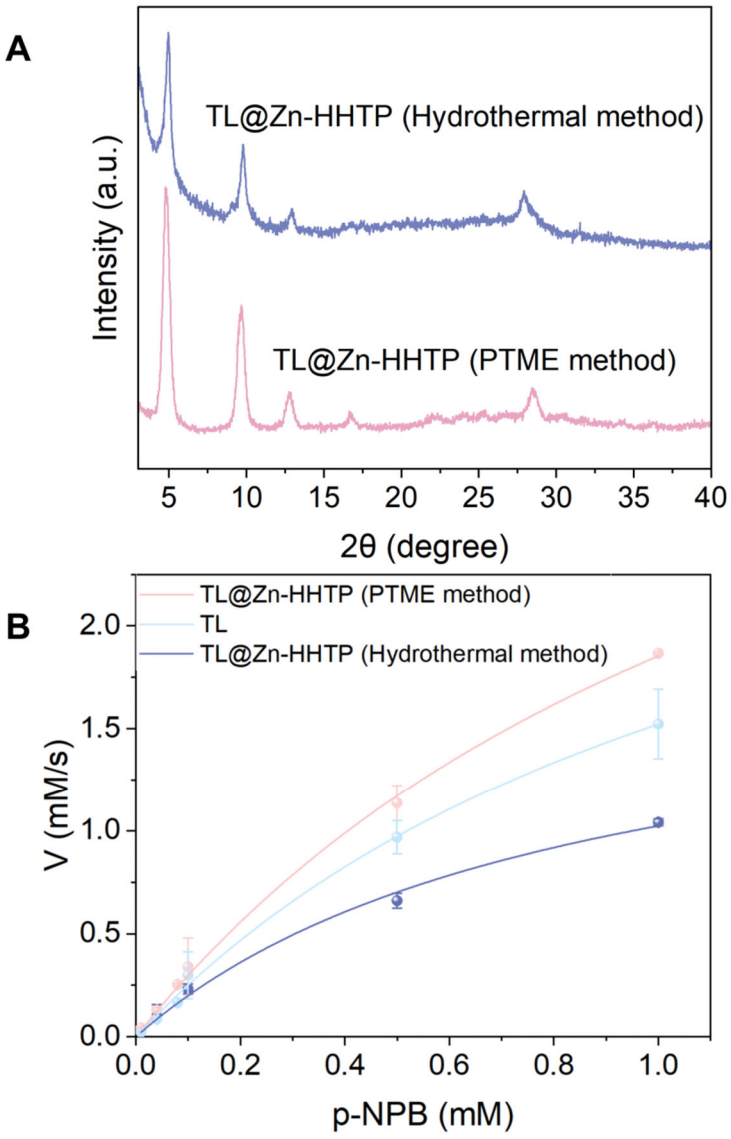

Figure S20. (A) Comparison of the PXRD of TL@Zn-HHTP synthesized by hydrothermal and PTME methods. (B) Plot of reaction velocity, V, against substrate [p-NPB] for TL@Zn-HHTP (hydrothermal method), TL@Zn-HHTP (PTME method) and TL. The error bars are representative of the standard deviation of the triplicates. The dosages of TL (5 μg/mL) were kept the same in each trial.

Supplementary References

[1] J. Y. Choi, M. Stodolka, N. Kim, H. T. B. Pham, B. Check and J. Park, *Chem*, 2023, **9**, 143-153.